WORKING PAPER
2006-05

Resource
Economics
and Policy Analysis
(REPA)
Research Group

Department of Economics
University of Victoria

Network Constrained Wind Integration: An Optimal Cost Approach

Jesse D. Maddaloni, Andrew M. Rowe and G. Cornelis van Kooten

November 2006

REPA Working Papers:

2003-01 – Compensation for Wildlife Damage: Habitat Conversion, Species Preservation and Local Welfare (Rondeau & Bulte)
2003-02 – Demand for Wildlife Hunting in British Columbia (Sun, van Kooten, & Voss)
2003-03 – Does Inclusion of Landowners' Non-Market Values Lower Costs of Creating Carbon Forest Sinks? (Shaikh, Suchánek, Sun, and van Kooten)
2003-04 – Smoke and Mirrors: The Kyoto Protocol and Beyond (van Kooten)
2003-05 – Creating Carbon Offsets in Agriculture through No-Till Cultivation: A Meta-Analysis of Costs and Carbon Benefits (Manley, van Kooten, Moeltner, and Johnson)
2003-06 – Climate Change and Forest Ecosystem Sinks: Economic Analysis (van Kooten and Eagle)
2003-07 – Resolving Range Conflict in Nevada? The Potential for Compensation via Monetary Payouts and Grazing Alternatives (Hobby and van Kooten)
2003-08 – Social Dilemmas and Public Range Management: Results from the Nevada Ranch Survey (van Kooten, Thomsen, Hobby, and Eagle)
2004-01 – How Costly are Carbon Offsets? A Meta-Analysis of Forest Carbon Sinks (van Kooten, Eagle, Manley, and Smolak)
2004-02 – Managing Forests for Multiple Tradeoffs: Compromising on Timber, Carbon and Biodiversity Objectives (Krcmar, van Kooten, and Vertinsky)
2004-03 – Tests of the EKC Hypothesis using CO2 Panel Data (Shi)
2004-04 – Are Log Markets Competitive? Empirical Evidence and Implications for Canada-U.S. Trade in Softwood Lumber (Niquidet and van Kooten)
2004-05 – Conservation Payments under Risk: A Stochastic Dominance Approach (Benítez, Kuosmanen, Olschewski and van Kooten)
2004-06 – Modeling Alternative Zoning Strategies in Forest Management (Krcmar, Vertinsky, and van Kooten)
2004-07 – Another Look at the Income Elasticity of Non-Point Source Air Pollutants: A Semiparametric Approach (Roy and van Kooten)
2004-08 – Anthropogenic and Natural Determinants of the Population of a Sensitive Species: Sage Grouse in Nevada (van Kooten, Eagle, and Eiswerth)
2004-09 – Demand for Wildlife Hunting in British Columbia (Sun, van Kooten, and Voss)
2004-10 – Viability of Carbon Offset Generating Projects in Boreal Ontario (Biggs and Laaksonen-Craig)
2004-11 – Economics of Forest and Agricultural Carbon Sinks (van Kooten)
2004-12 – Economic Dynamics of Tree Planting for Carbon Uptake on Marginal Agricultural Lands (van Kooten) (Copy of paper published in the Canadian Journal of Agricultural Economics 48(March): 51-65.)
2004-13 – Decoupling Farm Payments: Experience in the US, Canada, and Europe (Ogg & van Kooten)
2004–14 – Afforestation Generated Kyoto Compliant Carbon Offsets: A Case Study in Northeastern Ontario (Jeff Biggs)
2005–01 – Utility-scale Wind Power: Impacts of Increased Penetration (Pitt, van Kooten, Love and Djilali)
2005–02 – Integrating Wind Power in Electricity Grids: An Economic Analysis (Liu, van Kooten and Pitt)

2005–03 – Resolving Canada-U.S. Trade Disputes in Agriculture and Forestry: Lessons from Lumber (Biggs, Laaksonen-Craig, Niquidet and van Kooten)
2005–04 – Can Forest Management Strategies Sustain The Development Needs Of The Little Red River Cree First Nation? (Krcmar, Nelson, van Kooten, Vertinsky and Webb)
2005–05 – Economics of Forest and Agricultural Carbon Sinks (van Kooten)
2005–06 – Divergence Between WTA & WTP Revisited: Livestock Grazing on Public Range (Sun, van Kooten and Voss)
2005–07 – Dynamic Programming and Learning Models for Management of a Nonnative Species (Eiswerth, van Kooten, Lines and Eagle)
2005–08 – Canada-US Softwood Lumber Trade Revisited: Examining the Role of Substitution Bias in the Context of a Spatial Price Equilibrium Framework (Mogus, Stennes and van Kooten)
2005–09 – Are Agricultural Values a Reliable Guide in Determining Landowners' Decisions to Create Carbon Forest Sinks?* (Shaikh, Sun and van Kooten) *Updated version of Working Paper 2003-03
2005–10 – Carbon Sinks and Reservoirs: The Value of Permanence and Role of Discounting (Benitez and van Kooten)
2005–11 – Fuzzy Logic and Preference Uncertainty in Non-Market Valuation (Sun and van Kooten)
2005–12 – Forest Management Zone Design with a Tabu Search Algorithm (Krcmar, Mitrovic-Minic, van Kooten and Vertinsky)
2005–13 – Resolving Range Conflict in Nevada? Buyouts and Other Compensation Alternatives (van Kooten, Thomsen and Hobby) *Updated version of Working Paper 2003-07
2005–14 – Conservation Payments Under Risk: A Stochastic Dominance Approach (Benítez, Kuosmanen, Olschewski and van Kooten) *Updated version of Working Paper 2004-05
2005–15 – The Effect of Uncertainty on Contingent Valuation Estimates: A Comparison (Shaikh, Sun and van Kooten**)**
2005–16 – Land Degradation in Ethiopia: What do Stoves Have to do with it? (Gebreegziabher, van Kooten and.van Soest)
2005–17 –The Optimal Length of an Agricultural Carbon Contract (Gulati and Vercammen)
2006–01 – Economic Impacts of Yellow Starthistle on California (Eagle, Eiswerth, Johnson, Schoenig and van Kooten)
2006–02 – The Economics of Wind Power with Energy Storage (Benitez, Dragulescu and van Kooten)
2006–03 – A Dynamic Bioeconomic Model of Ivory Trade: Details and Extended Results (van Kooten)
2006–04 –The Potential for Wind Energy Meeting Electricity Needs on Vancouver Island (Prescott, van Kooten, and Zhu
2006–05 – Network Constrained Wind Integration: An Optimal Cost Approach (Maddaloni, Rowe, and van Kooten)

For copies of this or other REPA working papers contact:

REPA Research Group
Department of Economics
University of Victoria PO Box 1700 STN CSC Victoria, BC V8W 2Y2 CANADA
Ph: 250.472.4415
Fax: 250.721.6214
http://repa.econ.uvic.ca

Network Constrained Wind Integration: An Optimal Cost Approach

Jesse D. Maddaloni [a,*], Andrew M. Rowe [a], G. Cornelis van Kooten [a,b]

[a] Institute for Integrated Energy Systems, Department of Mechanical Engineering,
University of Victoria, PO Box 3055 STN CSC,
Victoria, BC, Canada, V8W 3P6
[b] Department of Economics, University of Victoria, PO Box 1700, STN CSC,
Victoria BC, Canada, V8W 2Y2

DRAFT: October 20, 2006

Abstract

Planning electricity supply is important because power demand continues to increase while there is a concomitant desire to increase reliance on renewable sources. Extant research pays particular attention to highly variable, low-carbon energy sources such as wind and small-scale hydroelectric power. Models generally employ only a simple load levelling technique, ensuring that generation meets demand in every period. The current research considers the power transmission system as well as load levelling. A network model is developed to simulate the integration of highly variable non-dispatchable power into an electrical grid that relies on traditional generation sources, while remaining within the network's operating constraints. The model minimizes a quadratic cost function over two periods of 336 hours, with periods representing low (summer) and high (winter) demand, subject to various linear constraints. The model is numerically solved using Matlab and GAMS software environments. Results indicate that, even for a grid heavily dependent on hydroelectricity, the addition of wind power can create difficulties, with system costs increasing with wind penetration, sometimes significantly.

Keywords*:* Electric networks; optimal power flow; wind power; intermittent sources.

Acknowledgements

The authors would like to thank Matt Schuett, Justin Blanchfield, Pablo Benítez, Ned Djilali, Lawrence Pitt, Alan Tucker and Peter Wild for their contributions to this work. Funding support from the B.C. Ministry of Mines and Petroleum Resources and SSHRC Grant #410-2006-0266 is gratefully acknowledged.

Nomenclature

A	Slope of the linear cost function	[CAD/MWh]
B	Cost intercept of the linear cost function	[CAD/MWh]
c	Cost of generation	[CAD/MWh]
Cost	Total cost of generation for full period T	[CAD]
Demand	Power demand at a bus	[MW]
G	Power generation at a bus	[MW]
H	Height	[m]
K	Loss factor for a bus connector	[-]
L	Power loss across a bus connector	[MW]
P	Power entering or leaving a bus connector	[MW]
S	Power consumption at a bus	[MW]
Sink	Power sink at a bus, due to excess generation	[MW]
Δt	Time step	[hr]
v	Wind speed	[m/s]
β	Surface shear factor	[-]

Subscripts

capacity	The nameplate capacity of a generator
data	The location where wind data is measured
Gen	The total number of generator buses
hub	The hub of a wind turbine
i, j, h, l	Bus indices
k, d, n	Generator bus indices
RD,full	A value associated with a full generator ramp down
RU,full	A value associated with a full generator ramp up
t	Discrete time index
T	Total time steps
α	Connection index

1. Introduction

Global electricity demand is rapidly increasing as developed nations continue to expand and developing nations grow even faster [1, 2]. Satisfying this demand is a central issue for national decision makers and system operators. Further, while meeting the growing demand, there is increasing pressure to reduce reliance on fossil fuels, thereby reducing or slowing emissions of carbon dioxide into the atmosphere. These concerns are augmented by the need to ensure supply security.

Modeling electricity generation and consumption commonly involves a simple load levelling technique that ensures generation satisfies demand during all periods – a simple energy balance [3]. Load levelling neglects the actual transmission network that moves power from the generation sites to user locations. In practice, a utility must consider both the transmission network and load levelling, guaranteeing that demand is met and that the existing transmission system is capable of moving the power.

Optimizing the energy balance between demand and generation under various network constraints is known as an optimal power flow (OPF) solution. The OPF problem has been solved for AC networks using a variety of optimization algorithms [4-8], with active power, reactive power and bus complex voltages the major control variables. Bus power balances are considered for both active and reactive power, as well as cable admittance (loss), and constitute the equality constraints that are a network's power flow equations. OPF inequality constraints typically correspond to equipment ratings and recommended practices of electric transmission. Researchers generally minimize either generation cost or system loss [4-8], with the majority focusing on the convergence properties of the optimization algorithms. This research provides a

description of the OPF problem and solution methods, but fails to model the behavior of both traditional and new generation technologies. By optimizing the OPF problem while considering non-traditional electricity generators, it is possible to shed light on the cost tradeoffs that occur when these new technologies are incorporated into an established and heavily constrained network.

The focus in this paper is to create a network model that simulates the behavior of both highly variable (wind) and traditional generation (thermal plants, large scale hydro), while also solving the optimal power flow problem under network constraints. A direct concern is to estimate the cost of electricity generation for utilities and governments, and analyze the cost tradeoffs when installing renewable and intermittent generation capacity.

A disadvantage of low carbon energy sources such as wind and wave energy is that they can be highly variable, and the prediction of when these sources will produce specific amounts of power can be inaccurate. Electricity demand throughout a day is semi-predictable, and existing generators and networks are generally able to follow this trend easily. When large amounts of unpredictable power enter a transmission network, say from a wind farm, then system operators can only rely on wind forecasting to know when they must ramp existing generators up or down to balance the remaining unmet load. The speed at which intermittent wind generation ramps up and down forces the existing generators to ramp much faster than they would in the absence of intermittent generation.

Due to increased ramping of existing thermal facilities, a significant decrease in operating efficiency during part load operation can occur. The decrease in efficiency corresponds to an increase in fuel consumption (on a per unit energy output basis) and

thus an increase in carbon dioxide emission intensity. Therefore, the introduction of intermittent and unpredictable sources into a previously thermal dominated generation mix may not substantially reduce the net production of CO_2 within the system [9]. Analyzing these tradeoffs in emissions, as well as tradeoffs in cost and reliability, is the motive for the development of the current network model.

2. Nodal Network Model

Since the current research involves the grid-integration of renewables, it is important to note the differences between dispatchable and non-dispatchable generation. *Dispatchable* electricity generation refers to facilities that are able to increase or decrease output when requested, or dispatched to do so. This is the case for fossil-fuel power plants, nuclear plants and hydroelectric facilities with storage reservoirs. *Non-dispatchable* electricity generation refers to facilities where the power output cannot be arbitrarily controlled; the power can be curtailed to be lower than that available, but the facility cannot be dispatched to ramp up when generation is requested. Non-dispatchable facilities include run-of-river hydroelectric, wind, wave, solar, tidal and cogeneration facilities that provide space heating.

As a consequence, the major operational assumptions of the current network model are as follows:

1. Electricity production must always satisfy demand.
2. At any instant in time, a bus connection must be unidirectional; power can only flow in one direction across a cable. Bidirectional flow across a connection is possible, just not simultaneously.
3. Dispatchable generation is constrained by the ramp rate.

4. Non-dispatchable generation is considered ‘must run’, but truncation is allowed under certain circumstances of excess generation.
5. The power across each cable is constrained.
6. Cost of generation will vary linearly as a function of capacity factor.

The network model is composed of geographically arranged buses, with each bus connected to various other buses using links. Each bus represents a transmission network substation, and the bus linkages represent the transmission cables between each station. Each bus may have its own local generation or demand, while also allowing power to pass through it en route to other consuming buses. These assumptions in conjunction with the convention shown in Figure 1 lead to the bus power balance equation:

$$\sum_{j}^{links} P_{i,j,t} + S_{i,t} + Sink_{i,t} - G_{i,t} = 0 \quad \forall \quad i = 1,2,...,buses \quad \& \quad t = 1,2,...,T \,, \qquad (1)$$

where S denotes power consumption, *Sink* refers to power export or storage, and G denotes power generation. Equation (1) constitutes a separate constraint for each bus i, and holds for every time period t. The bus power balance equation accounts for load levelling and transmission, and ensures that demand is met at each bus for each time. The summation term accounts for all connections between buses j ($j=1,2,...,links$) and bus i.

The power moving from a bus across a link is defined positive leaving the bus as indicated by Figure 1, where a visual representation of this convention is employed. The $P_{i,j,t}$ term in Figure 1 shows the power leaving bus i for bus j at time t. The connection between nodes i and j at time t is considered in Figure 2. Since power is defined as positive when leaving a bus, Figure 2 shows the two terms $P_{i,j,t}$ and $P_{j,i,t}$ entering the link from different directions. The unidirectional constraint on the linkage specifies that one of the $P_{i,j,t}$ or $P_{j,i,t}$ terms must always be positive, while the other must always be negative.

The directional convention in Figure 2 leads to the linkage power balance equation:

$$P_{i,j,t} = -P_{j,i,t} \tag{2}$$

Equation (2) does not account for power loss across a transmission linkage. This is neglected to simplify the network and allow the optimization problem to be formulated with linear constraints. The simultaneous solution of Equations (1) and (2) ensures that power generation will always be sufficient to meet demand ($\sum_{i}^{nodes} S_i$) in each time period.

Power loss across a linkage can be considered by re-writing Equation (2) as $P_{i,j,t} + P_{j,i,t} = L_{\alpha,t}$, where $L_{\alpha,t}$ is the power loss across linkage α at time t. An additional non-linear constraint must also be incorporated to calculate the transmission loss, which could be calculated by multiplying the maximum power entering the linkage by a constant loss factor K ($L_{\alpha,t} = \max\{P_{i,j,t}, P_{j,i,t}\} \cdot K_{\alpha}$). To calculate loss using this approach, the loss factor K must be multiplied by the power term entering the linkage (or the maximum or positive power term) to ensure that power is reduced along the direction of transmittal. If the loss was calculated using the minimum or negative power term then power would increase along the direction of transmittal, and power would be gained from transmission and not lost. Including a discontinuous 'max' operator as a network constraint adds to the complexity of finding an optimum solution, and, for some solvers, this requires too short a time period for which it is possible to obtain feasible solutions. The discontinuous loss constraint was removed from the formulation for this paper in order to make the constraint set purely linear and allow an optimal solution to be found over longer time periods.

The power moving across each linkage, both positive and negative, must be constrained so that transmitted power does not exceed the link capacity. The link capacity constraints are written as follows:

$$P_{i,j,t} \leq P_{\alpha,\max} \tag{3}$$

$$P_{i,j,t} \geq -P_{\alpha,\max} \tag{4}$$

For dispatchable generating sources, power generation is limited to the maximum output available from a facility:

$$G_{d,t} \leq G_{d,capacity} \quad \forall\, d = 1, \ldots, \text{non-dispatchable generators.} \tag{5}$$

Dispatchable generation facilities are also ramp-rate constrained, so that the increase or decrease in power output over a single time step is limited to be within the operating ability of the facility. The respective ramp-up and ramp-down constraints are:

$$\frac{G_{d,t} - G_{d,(t-1)}}{\Delta t} \leq \frac{G_{d,capacity}}{\Delta t_{RU,full}} \tag{6}$$

$$\frac{G_{d,t} - G_{d,(t-1)}}{\Delta t} \geq -\frac{G_{d,capacity}}{\Delta t_{RD,full}} \tag{7}$$

where the terms $\Delta t_{RU,full}$ and $\Delta t_{RD,full}$ denote the time required for a facility to ramp up from zero to full capacity and the time to ramp down from full capacity to zero, respectively. The numerators on the left hand sides of Equations (6) and (7) are the changes in power output that occur during a time step. The right hand sides of (6) and (7) are the limits by which a facility can either increase or decrease output over a single time step. Non-dispatchable generation is not ramp-rate constrained, but is considered *must run*. This constrains the network so that any power available from a non-dispatchable source must be used by the network during that time period:

$$G_{n,t} = G_{n,t,available} \ \forall\, n = 1, \ldots, \text{non-dispatchable generators.} \tag{8}$$

Finally, generation from all facilities, dispatchable or non-dispatchable, can never be negative:

$$G_{k,t} \geq 0 \ \forall\, k = 1, \ldots, \text{generators.} \tag{9}$$

The power consumption at a typical bus will simply follow the consumer demand at that bus (substation) for the given time period *t*. It is assumed that demand at each bus is known *apriori*. The nodal consumption constraint is thus

$$S_{i,t} = Demand_{i,t} \tag{10}$$

Due to the *must run* constraint (8) and the ramp-down constraint (7), there may exist some time periods when generation is forced to exceed demand. If there is no sink to absorb this excess, the model will not find a feasible solution. This requires one or more buses to have the potential to either consume power for storage or export power to a location outside the network. Both options take the form of added (sink) constraints:

$$Sink_{i,t} \geq 0 \tag{11}$$

$$Sink_{i,t} \leq Sink_{capacity}, \tag{12}$$

where a bus may have a sink term that is able to increase in the event of excess generation. The amount of excess power that can be absorbed is limited by the rate of storage in Equation (12), but not with respect to the maximum amount of energy stored over the full time period *T*, $\sum_{t}^{T}\left(Sink_{i,t} \cdot \Delta t\right)$. Future research will focus on the inclusion of such an energy constraint, as well as the round-trip storage efficiencies when using this energy to satisfy demand at some future time. If excess generation occurs during a time step, dispatchable generators may be able to absorb the excess by loading the network,

instead of adsorption occurring at an additional sink. The possibility of loading the network with a negative generation term has not been considered in this paper.

The objective is to minimize the cost of generation over each period T, as follows:

$$Minimize\,Cost = \sum_{t}^{T}\sum_{k}^{Gen} c_{k,t} \cdot G_{k,t} \tag{13}$$

In (13), the cost coefficients (c) are a function of the level of generation (G) for dispatchable generators, but are constant for non-dispatchable generators. For dispatchable generation, the cost coefficients are assumed to follow a linear trend with respect to the part-load operation of the facility:

$$c_{d,t} = A_d \cdot \left(\frac{G_{d,t}}{G_{d,capacity}} \right) + B_d \,, \tag{14}$$

where the fractional term ($G_{d,.t} / G_{d,capacity}$) represents the normalized part-load operation of (dispatchable) generator d. The slope A_d and the vertical intercept B_d of the linear approximation can be determined using the efficiency of a generator during part-load operation, and the cost per unit input energy into the facility. Actual values for A_d and B_d are discussed in the network parameterization section. The slope term is typically negative, resulting in an increased cost per unit output when operating below the full capacity of the generator.

Optimization of objective (13) subject to constraints (1) through (12) is performed using GAMS [10]. The problem is a discrete dynamic quadratic program with linear constraints, and is solved using the Minos solver. In the current application, GAMS solves the optimal control model over a period of two weeks at an hourly resolution (although any length of time and time step could be chosen), and Matlab is used to feed parameters to the GAMS routine for each hour. Matlab is the main shell for the network

model and is used to loop the GAMS optimization as well as perform general data management. Data such as nodal demand and wind speeds are input into Matlab, the m-file then calls GAMS for each optimization and returns the solution.

Due to the discrete dynamic operation of the model, starting values are required for each optimization period so that state equations (6) and (7) may be initially defined. For the first optimization period, the starting activities are set as the optimal static solution of the first time period. For subsequent optimization periods, the starting activities are the final activities from the previous optimization period.

3. Network Parameterization

A small network is used to validate the constrained operation of the model and to provide insights regarding the model's capabilities. As shown in Figure 3, the test grid is composed of 7 buses (labelled 1 through 7) and 9 linkages (labelled *a* through *i*). The algebraic terms for power moving out from each bus are indicated in Figure 3. All solutions employ 336 periods, each representing one hour over two weeks, with the optimization assuming rational expectations – demand is known and non-dispatchable power is perfectly predicted. The network is formulated to represent a simplified version of the existing network on Vancouver Island, a 500 km long island off the west coast of British Columbia, Canada.

Buses 1, 2, 3, 5, 6 and 7 make up the Vancouver Island network, and bus 4 is a BC mainland bus, connected to the island network via linkage *d*. Linkage *d* is modeled as a high voltage submarine cable with the capacity to transmit 1300 MW either to or from the Island. The required export/storage sink (as described by Equations 11 and 12) is placed at bus 4 so that any excess generation can be exported to the BC mainland. Power

is consumed at buses 1, 2, 3, 5, 6 and 7 and the mainland bus 4 consumes power for export only.

Demand data for Vancouver Island were provided by BC Hydro [11] in the form of a conglomerated hourly load for the entire Island for 2003. Two 336 hour demand profiles are used to demonstrate the network operation over both high (*winter*) and low (*summer*) demand periods. The high demand profile is the actual Vancouver Island demand for December 18-31, 2003, while the low demand profile is the actual demand for July 9-22, 2003. The winter and summer demand profiles are shown in Figures 4 and 5, and have respective energy demands of 508 GWh and 366 GWh. The dispersion of Island residential and commercial demand among the six Island buses is performed using population and proximity of local substations to each of the buses. Industrial demand was nearly constant at 370 MW, mostly from Island pulp mills, and was dispersed among the six buses according to the proximity of pulp facilities to the buses.

Buses 1, 2, 3, 4 and 7 all generate power, with thermal generators located at buses 1 and 4. Large scale hydroelectric generators are located at buses 1, 3, 4 and 7, and wind generation is located at bus 2. The placement and type of all generators is illustrated as a network diagram in Figure 3. The thermal generator at node 1 is a combined-cycle, natural gas-steam unit with a capacity of 290 MW. The thermal generator at bus 4 is a simple cycle natural gas unit, with a capacity of 400 MW. The hydroelectric generators at buses 1, 3, 4 and 7 have capacities of 237, 57, 900 and 170 MW, respectively. The generator types and capacities have all been chosen to represent the actual generation capability on Vancouver Island.

The only generators that are ramp rate constrained are the two thermal generators.

Both can ramp up from zero to their full capacity in one hour, but can only ramp down half of their capacity in one hour. All hydroelectric generators are modeled without ramp-rate constraints.

The constants A_d and B_d (Equation 15) that describe the variable cost of the dispatchable generators are listed in Table 1. For the two thermal plants, the constants are calculated using a natural gas price of 6.67 CAD/GJ (6.20 USD/MMBtu) [12], and part load efficiencies obtained from [13] and [14]. For the thermal power plants, only fuel costs are taken into account, with operating, maintenance and capital costs considered fixed ('water under the bridge'). For the (dispatchable) hydro facilities, the constants A_d and B_d are calculated using water license rental rates associated with power production for 2006 [15], which can be regarded as fuel costs. The rental rates are 1.086 CAD per generated MWh, and 0.006 CAD per 1000 m^3 of throughput water. These dollar amounts are used in conjunction with part load efficiency data for a Francis hydroelectric turbine [16], specific head heights for Vancouver Island facilities and maximum flow rates to approximate operating cost over the range of generator output. From Table 1, the cost of the hydro generation is a fraction of the cost of thermal generation. This is because fossil fuel costs are high and water license rates for hydro facilities are low, while operating, maintenance and capital costs for all facilities are neglected.

Bus 2 encompasses the non-dispatchable generator, simulating multiple wind turbines at a single location. This simulation assumes that all turbines experience the same wind speed at the same time, neglecting spatial dispersion of generation across the area of the turbine farm. The 336 data points (hourly wind speed over two weeks) used for this exercise were observed at Jordan Ridge on Vancouver Island (Lat: 48 25 48,

Long: -124 03 45) from August 19 to September 1, 2001, at a height of 30 m above the site elevation of 671 m [17]. This two-week wind profile was chosen because it includes both maximum and minimum annual wind speeds. Measured wind speeds at this location are indicated in Figure 6, as is the power generated from a single Enercon 70 [18] wind turbine with a rated capacity of 2.05 MW. The wind speed is measured at 30 m, but was scaled as follows to correspond to a turbine hub height of 113 m [19]:

$$v_{hub} = \left(\frac{H_{hub}}{H_{data}} \right)^{\beta} \cdot v_{data} \tag{15}$$

The terms v_{hub} and v_{data} in (15) represent the wind speed at the hub height (H_{hub}) and data measurement height (H_{data}), respectively. In (15), β is the surface shear factor and depends on the ground cover at the turbine location. For this exercise, the shear factor was chosen to be 0.14, the mean value between short grasses and low vegetation [20].

All simulation results presented in this paper will use the same two week wind speed profile in order to facilitate better comparisons among all the scenarios. Wind generation is modeled with zero cost, although some analyses will include an amortized capital cost of the wind farm installation.

Each of the nine bus connections (*a* through *i*) of the simulated network have a constraint placed on the amount of power that can be sent across them. Three cable constraint scenarios have been created – unconstrained, constrained and actual constraint cases. The cable capacities for each link and each of the three scenarios are listed in Table 2. For all simulations, the transmission capacity on link *d* is 1300 MW, representing the actual transmission capacity of the submarine cable connecting Vancouver Island to the BC mainland. For the unconstrained scenario, all line capacities are set to 2000 MW except for link *d*. Cables *a* and *c* connect the wind farm to the

network; if the peak power generation from the wind farm exceeds 2000 MW, the capacities on these two cables are set to the peak wind farm output plus 20%. The constrained scenario uses actual line capacities for the Vancouver Island grid, with the same variable capacity criteria set out for cables *a* and *c*. The actual constraint scenario again uses the actual line capacities for the Vancouver Island grid, but now the capacities of cables *a* and *c* stay constant at 60 and 100 MW, respectively.

Dependant variables for this optimal power flow problem include all 18 of the link power terms ($P_{i,j}$), the six levels of power generation from the six dispatchable generators, and the export/storage sunk power at bus 4.

4. Optimal Power Flow Results

Wind power penetration is used to measure the growth of a wind farm installation. It is defined as the wind farm's name-plate capacity normalized with respect to peak network demand, which is 1971 MW. For example, a 10% wind power penetration implies a wind farm capacity of 197.1 MW, or 96 installed Enercon E70 turbines rated at 2.05 MW each. Two forms of wind penetration into a network can occur: power penetration and energy penetration. Power penetration is a measure of the instantaneous peak power that enters a network at a given time, while energy penetration is a measure of how much wind energy enters a network over a specified period.

The maximum allowable power penetration entering the network depends on the cable capacities that link the wind farm to the network, as well as on the demand at the bus where the wind farm is located. The amount power transmitted to or from the bus where the wind farm is located is the power remaining after the local demand has been subtracted from the wind generation (positive outgoing and negative incoming). A large

demand at the wind farm bus will allow a larger power penetration, if the periods of high demand and high wind generation coincide. For the winter demand profile, wind power penetration can rise to 9.9% for the actual constrained scenario, and 127.3% for both the unconstrained and constrained scenarios. For the summer demand profile, wind power penetration can rise to 9.6% for the actual constrained scenario, and 113.2% for both the unconstrained and constrained scenarios. The low penetration for the actual line capacities scenario exemplifies the need for additional transmission capacity if wind power penetration into the network is to exceed 10%.

The *energetic capacity factor* is a ratio of produced energy over a given time period divided by the maximum amount of energy that that capacity could provide over the same time period. The wind profile has an energetic capacity factor of 22.7% over the two winter weeks considered in the model. If truncation of wind generation is allowed, a higher power penetration can be introduced into the network without raising transmission capacities; however, truncation will result in a drop in the capacity factor of the wind farm and a drop in the level of energy penetration into the network. The energetic capacity factor for the wind farm is shown in Figure 7 with respect to increasing wind power penetration (using the cable capacities of the actual constraint circumstance and the winter demand profile). As wind penetration increases to roughly 10%, the capacity factor stays constant at 22.7%, and no truncation of wind generation is required. Once the output of the wind farm reaches the limit of the cables connecting it to the network, a portion of the generation must be truncated and the capacity factor drops. Two capacity factor curves, one corresponding to a 100 MW capacity on cable *c* and the other to a 200 MW capacity on cable *c*, are shown in Figure 7. When the capacity of the cable

connecting the wind farm to the grid is raised, a larger portion of the wind energy can enter the network, resulting in the larger capacity factors seen in the figure. Increasing the capacity factor of the wind farm will increase the capacity factor of other (existing) generators in the network, leading to a reduced system generation cost.

The demand profiles for the network are less variable than the wind generation profile, with an average power demand of 76.7% of the maximum of 1971 MW during the winter period, and an average power demand of 79.4% of the maximum of 1372 MW during the summer period. A highly intermittent source partially supplying power for a more regular demand results in the existing generators in the network ramping up and down more frequently to balance the remaining load. This results in a drop in the capacity factors (but not always) for the existing generators as the size of the wind farm grows (see Figure 8). The existing dispatchable generators are modeled to have a higher cost at lower capacity. Therefore, a drop in the capacity factor directly increases the operating cost of the generators. All existing generators show a decline in capacity factor with increased wind penetration, except for the thermal generator at bus 1, which exhibits an increase in capacity factor for moderate wind penetrations. This increase in capacity factor for the relatively expensive thermal generator occurs because its operation is still required to meet demand at moderate wind penetration. The thermal facility has a lower cost when operated at a larger part load, so the optimal cost solution drives the capacity factor of the generator up until the net benefit of its high generation within the system becomes negative.

A load duration curve (LDC) is constructed by sorting demand over a certain period from maximum to minimum, thereby identifying the portion of demand that can

be met by base load. Base load is the portion of demand that remains constant throughout the period, with variations above base load demand to be met by load following or peaking generation sources. As wind penetration grows, the base load component of the network demand decreases, which can reduce the amount of time an existing generator can operate at a steady output. Six LDCs for winter and one for summer demand are shown in Figure 9. Different amounts of wind generation are subtracted from demand in the construction of the LDCs. The 'no wind' LDC shows the unreduced demand for the winter period, with a base load of 1000 MW. As wind penetration increases, more of the demand is satisfied with wind power, but the base load requirement falls. At 60% wind penetration, the base load requirement drops to zero, and the opportunity for a generator to remain at a constant generation level over the two-week period is eliminated. At penetrations above 60%, the LDCs become negative at the tail end of the duration, indicating that generation from the wind farm has exceeded demand and that export of power out of the network must occur. When demand is low and wind penetration is high, more excess wind generation occurs and a larger proportion must be exported, which is shown by the 100% wind penetration for the summer demand LDC (Figure 9). Figures 8 and 9 together show the decline of base load demand with increased wind penetration, which forces a drop in capacity factors for most generators, which will result in an increased operating cost of existing generators. The induced cost on existing generators from wind's variability will be discussed next.

Wind Induced Cost on Existing Generators

The hydro generator located at bus 3 is used to illustrate the effect that the introduction of wind-generated power has on the operating costs of existing generators.

The hydro generator has been modeled to cost a minimum of 1.0927 CAD/MWh at full operating capacity (denoted c_{FC}), and a maximum of 1.1281 CAD/MWh at zero operating capacity (denoted c_{ZC}). Thus it has a cost range of $c_R = c_{ZC} - c_{FC} = 0.0354$ CAD/MWh. The average cost of the generator with wind penetrating the network can then be defined marginally as a percentage of the cost range:

$$\overline{c}_M \equiv \frac{\overline{c}_W - \overline{c}_o}{c_R} \tag{16}$$

where $\overline{c}_M$ is the average marginal cost of the existing generator, $\overline{c}_W$ is the average cost of the generator with wind penetration and $\overline{c}_o$ is the average cost of the generator without any wind penetration. These costs and their range are small compared to the costs of a natural gas facility, but, by presenting results as a percentage of the cost range, it is still possible to provide insights into the potential increase in operating costs induced by wind penetration. The average marginal cost, $\overline{c}_M$, for the hydro generator at bus 3 is shown in Figure 10 with respect to increasing wind power penetration. The marginal cost is zero when no wind power enters the network. As wind penetration grows to 100% penetration, the marginal cost of the hydro generator rises to 60% of the full cost range. The induced marginal cost for the summer demand profile is larger than the induced cost for the winter profile due to less power absorption buffering the intermittency of the wind source in the network and because a lower capacity factor is expected of a generator during periods of low demand. When demand drops and wind generation remains the same, the capacity factors of existing generators drop further compared to high demand periods, resulting in greater variance and a higher operating cost. This is shown by the difference between the two curves in Figure 10.

System Costs

What happens to system costs as wind penetration grows? If per unit operating costs of generators do not increase as output falls relative to capacity, one would expect total system operating costs to decline linearly as wind penetration grows and wind power satisfies at zero cost the demand previously satisfied by existing generators. This is not the case, however, for at least two reasons. First, ramping constraints prevent thermal power plants from responding quickly enough to the availability of wind power to the grid. Second, as wind penetration grows, the costs of using extant generators to satisfy remaining demand rises, so system-wide costs decline at a declining rate, as illustrated in Figure 11. The data in Figure 11 correspond to the winter demand profile and the scenario where cable capacity is unconstrained. A certain cost to operate the system exists at zero wind penetration, where the entire demand is met by existing generators. As wind penetration grows, a portion of the demand previously met by existing generation is now satisfied by zero cost wind and the total system operating cost declines. As wind penetration becomes increasingly significant, the induced intermittency on existing generators also grows, increasing their specific cost and diminishing the benefit of introducing the large wind farm. However, all this ignores capital costs.

If capital costs related to the construction and installation of the wind farm are taken into account, total system operating costs rise as wind penetration increases, as also indicated in Figure 11. The capital cost for the wind farm is assumed to be 600 CAD per kW of installed wind capacity [9], and is amortized over 20 years at a discount rate of 10%. The annual amortized fee is then reduced by a fraction of (336/8760) to approximate a two-week amortized capital cost for the wind farm construction and installation. Including capital costs causes total system operating costs to more than

double as wind penetration goes from zero to 120%, compared to a decline of about one-third if capital costs are ignored.

When the capital cost of the wind farm installation is included, the increase in overall system operating cost indicates that adding wind capacity to the network can be distinctly detrimental. This can be partly attributed to the inexpensive existant generation mix for the network. A typical North American generating mix is predominantly thermal [13], unlike on Vancouver Island where hydroelectric dominates, supplying 70% of load. When considering fuel costs for a thermal-dominated generation mix, overall system operating cost will be significantly larger and the benefit of adding wind capacity to the system will be greater than indicated in Figure 10. Future work will focus on a range of generation mixtures to identify the impacts of both cost and emissions when adding wind capacity to a variety of networks and generation mixes.

5. Conclusions

In this paper, we formulated an optimal power flow model that considered the interaction between existing and new generation technologies under the constraint of an existing transmission network. The optimization problem was formulated as a quadratic program with linear constraints, solved over two-week periods using an hourly resolution and minimizing generation cost. The network model approximates the actual transmission network on Vancouver Island, British Columbia. Wind generation was introduced into the modeled network, coexisting with a generation mixture of natural gas thermal plants and large-scale hydroelectric facilities.

Results show that the wind farm capacity factor is limited due to transmission capacity constraints, and that the energetic capacity factor of the wind farm must decline

if penetration is to exceed 10%. If power penetration is to exceed 10% without a decline in capacity factor, transmission capacity to the Northern region of Vancouver Island must be increased. When wind power penetration exceeds 60% during peak demand periods, wind generation will exceed demand in some non-peak periods and power must be exported.

Using load duration curves, we showed that base-load generating potential falls with increased wind penetration, with base load eliminated entirely at 60% penetration in the case of winter demand. As wind penetration increases, the majority of existing generators in the network experience a drop in their capacity factor, leading to more frequent operation at part load and thereby a reduction in average operating efficiency. The fall in average efficiency leads to an increase in average operating cost for the existing generators.

Results also showed that system costs begin to decline rapidly as small amounts of zero-cost wind enter the network. As wind penetration grows, the average costs of the existing generators increase, and the benefit of introducing zero-cost wind into the system declines. For the Vancouver Island generation mix, system operating costs fall for the full range of wind penetration up to 120%. However, when the amortized capital cost of the wind installation was included, system costs increased for every wind penetration level, resulting in a net negative benefit throughout the entire penetration range.

The Vancouver Island network is dominated by hydroelectric power (70%), resulting in an inexpensive system generation costs at zero wind penetration – 0.7 Canadian cents per kilowatt-hour. However, when the capital cost of the wind farm was included in the analysis, the system costs increased significantly with respect to wind

penetration, with costs more than doubling at 120% wind penetration. If wind was to enter a thermal-dominated network, system generation costs would be substantially larger, and the effect of incorporating the capital cost of the wind farm would not be such an overriding component of the total increase in system costs.

Future research will need to expand the network model to consider more thermal generation. Future development of the model will also need to include storage at buses, such that non-dispatchable power can be stored from one time period to the next. Storage facilities will include rate constraints to limit the amount of power a system can absorb or produce during a single time step, with the inclusion of round-trip efficiencies and maximum storable energy. Minimum cut-off limits will also be included for dispatchable generators, so that a facility will stop generating power when its part-load output falls below a specified lower limit. The cost of generation for both dispatchable and non-dispatchable sources will also be augmented with operating and maintenance costs for the associated facility. Installation of additional transmission capacity can be made a decision variable in the model, so that associated capital costs will be included. This enables one to analyze the benefits and drawbacks of installing additional transmission capacity. These modifications are also important because they enable one to measure the costs of reducing CO_2 emissions, an important policy consideration.

References

1. EIA, International energy outlook 2005.

2. Asif M, Muneer T, Energy supply, its demand and security issues for developed and emerging economies. Renewable & Sustainable Energy Reviews 2005; Article in Press.

3. Kennedy S, Wind power planning: assessing long-term costs and benefits, Energy Policy 2005; 33: 1661-1675.

4. El Abiad A, Jaimes F, A method for optimum scheduling of power and voltage magnitude. IEEE Transactions on Power Apparatus and Systems 1969; PAS-88 No.4: 413-422.

5. Dommel H, Tinney W, Optimal power flow solutions. IEEE Transactions on Power Apparatus and Systems 1968; PAS-87: 1866-1876.

6. Sasson A, Combined use of the parallel and Fletcher-Powell non-linear programming methods for optimal load flows. IEEE Transactions on Power Apparatus and Systems 1969; PAS-88 No.10: 1530-1537.

7. Barcelo W, Lemmon W, Koen H, Optimization of the real-time dispatch with constraints for secure operation of bulk power systems. IEEE Transactions on Power Apparatus and Systems 1977; PAS-96 No.3: 741-757.

8. Talukdar S, Giras T, Kalyan V, Decompositions for optimal power flows. IEEE Transactions on Power Apparatus and Systems 1983; PAS-102 No.12: 3877-3884.

9. DeCarolis J, Keith D, The economics of large-scale wind power in a carbon constrained world. Energy Policy 2006; 34: 395 – 410.

10. Brooke A, Kendrick D, et al, GAMS. A User's Guide 2005, Washington, DC, GAMS Development Corporation.

11. BC Hydro, private communication, 2003.

12. DOE/EIA, Natural gas weekly update, April 20th 2004. http://tonto.eia.doe.gov/oog/info/ngw/ngupdate.asp

13. DOE/EIA, Assumptions for the annual energy outlook 2004 with projections to 2025, 2004.

14. Kim T S, Comparative analysis on the part load performance of combined cycle plants considering design performance and power control strategy, Energy 2004; 29: 71-85.

15. Ministry of Environment, Province of British Columbia, Annual water license rental

rates associated with power production, February 2006. http://www.env.gov.bc.ca/wsd/water_rights/water_rental_rates/cabinet/new_rent_structure_waterpower.pdf

16. RETScreen International, Natural Resources Canada, Francis turbine efficiency, 2004. http://www.retscreen.net/

17. BC Hydro, Wind Data Release #2, August 2004. http://www.bchydro.com/environment/greenpower/greenpower1764.html

18. Enercon, E70 technical data sheet, 2005. http://www.enercon.de/en/_home.htm

19. Auer P, Advances in Energy Systems and Technology 1978. Vol. 1. New York, Academic Press.

20. Institute for Energy Technology, HYDROGEMS, P.O. Box 40, NO-2027, Kjeller, Norway.

Table 1: Part-load cost parameters for dispatchable generators (Equation 15)

	A [CAD/MWh]	*B* [CAD/MWh]
Bus 1 Thermal	-25	90
Bus 4 Thermal	-25	70
Bus 1 Hydro	-0.0864	1.1886
Bus 3 Hydro	-0.0354	1.1281
Bus 4 Hydro	-0.0432	1.1373
Bus 7 Hydro	-0.0209	1.1109

Table 2: Network link capacities for the unconstrained, constrained and actual scenarios

	Cable Capacities [MW]		
Cable	Unconstrained	Constrained	Actual
a	2000 or higher	60 or higher	60
b	2000	320	320
c	2000 or higher	100 or higher	100
d	1300	1300	1300
e	2000	700	700
f	2000	610	610
g	2000	300	300
h	2000	650	650
i	2000	650	650

Figure 1

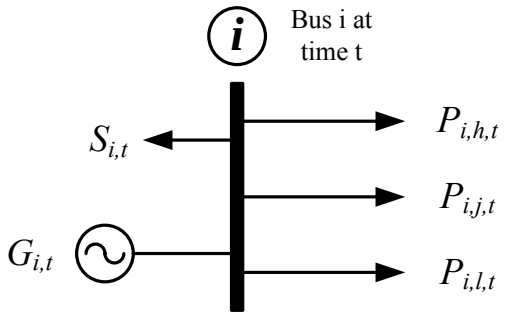

Figure 2

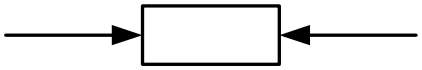

Figure 3

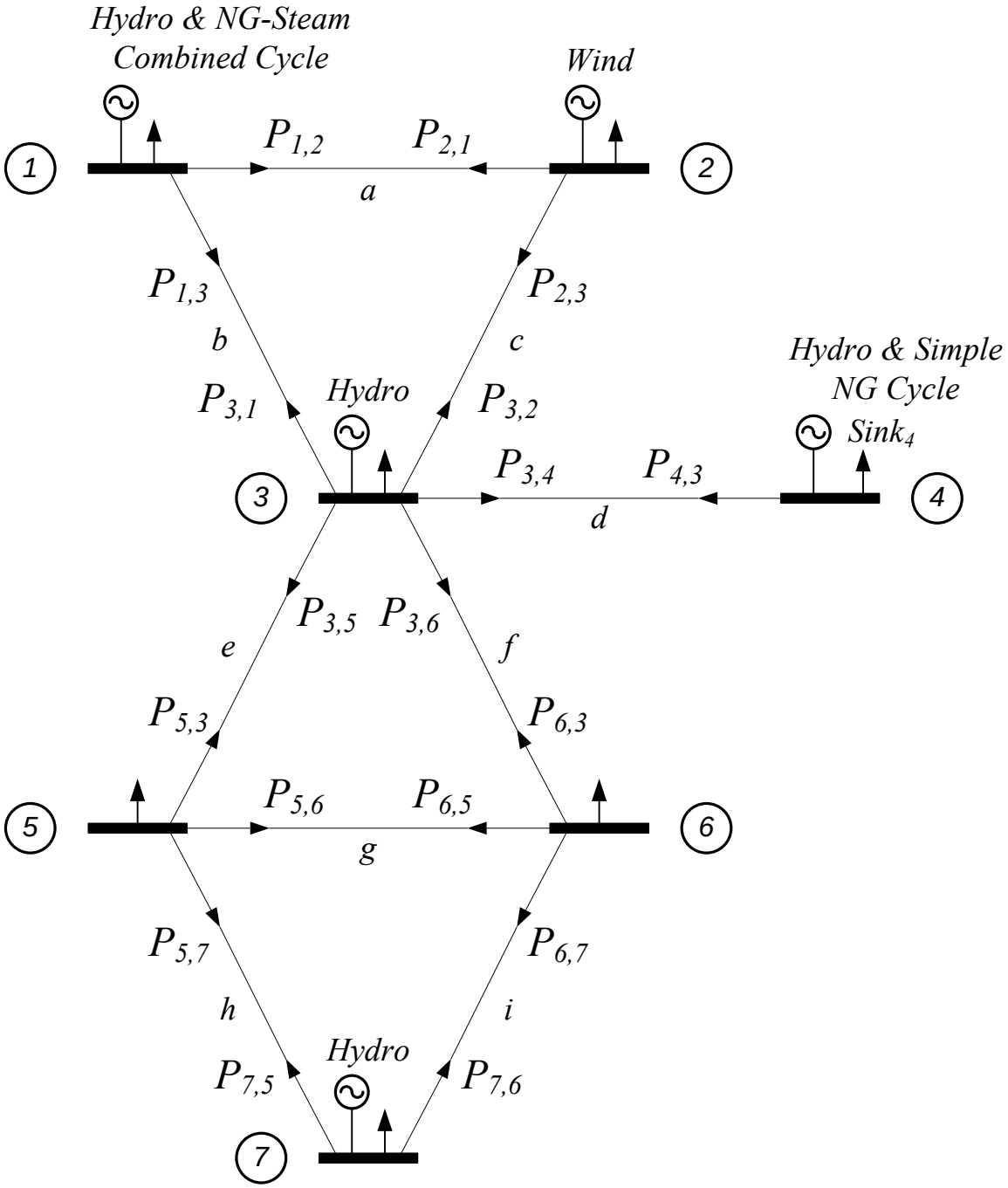
Hydro & NG-Steam Combined Cycle
Wind
Hydro & Simple NG Cycle
Hydro
Hydro
Sink4
1
2
3
4
5
6
7
P1,2
P2,1
a
P1,3
P2,3
b
c
P3,1
P3,2
P3,4
P4,3
d
P3,5
P3,6
e
f
P5,3
P6,3
P5,6
P6,5
g
P5,7
P6,7
h
i
P7,5
P7,6

Figure 4

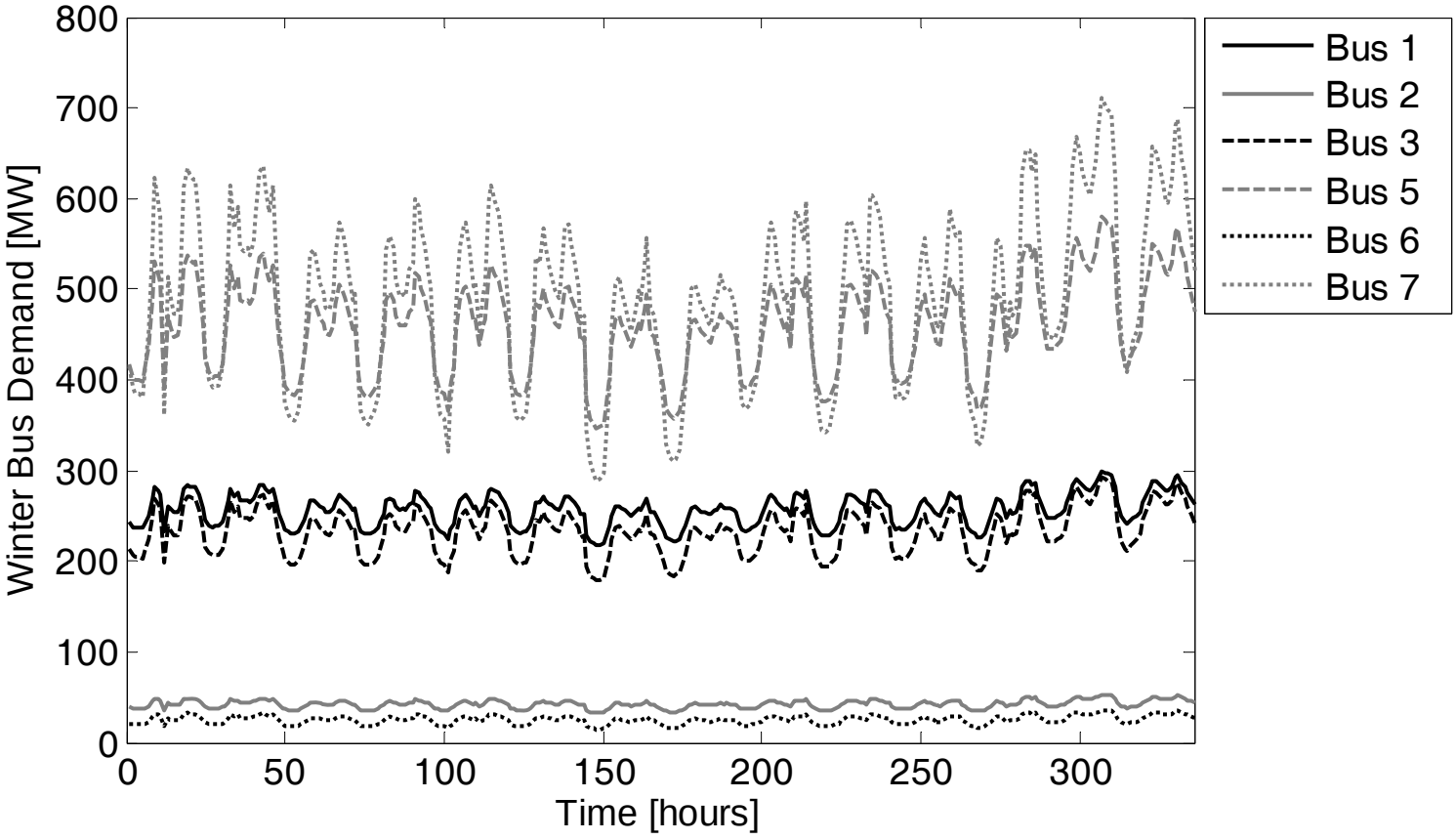
800
700
600
500
400
300
200
100
0
Winter Bus Demand [MW]
0
50
100
150
200
250
300
Time [hours]
Bus 1
Bus 2
Bus 3
Bus 5
Bus 6
Bus 7

Figure 5

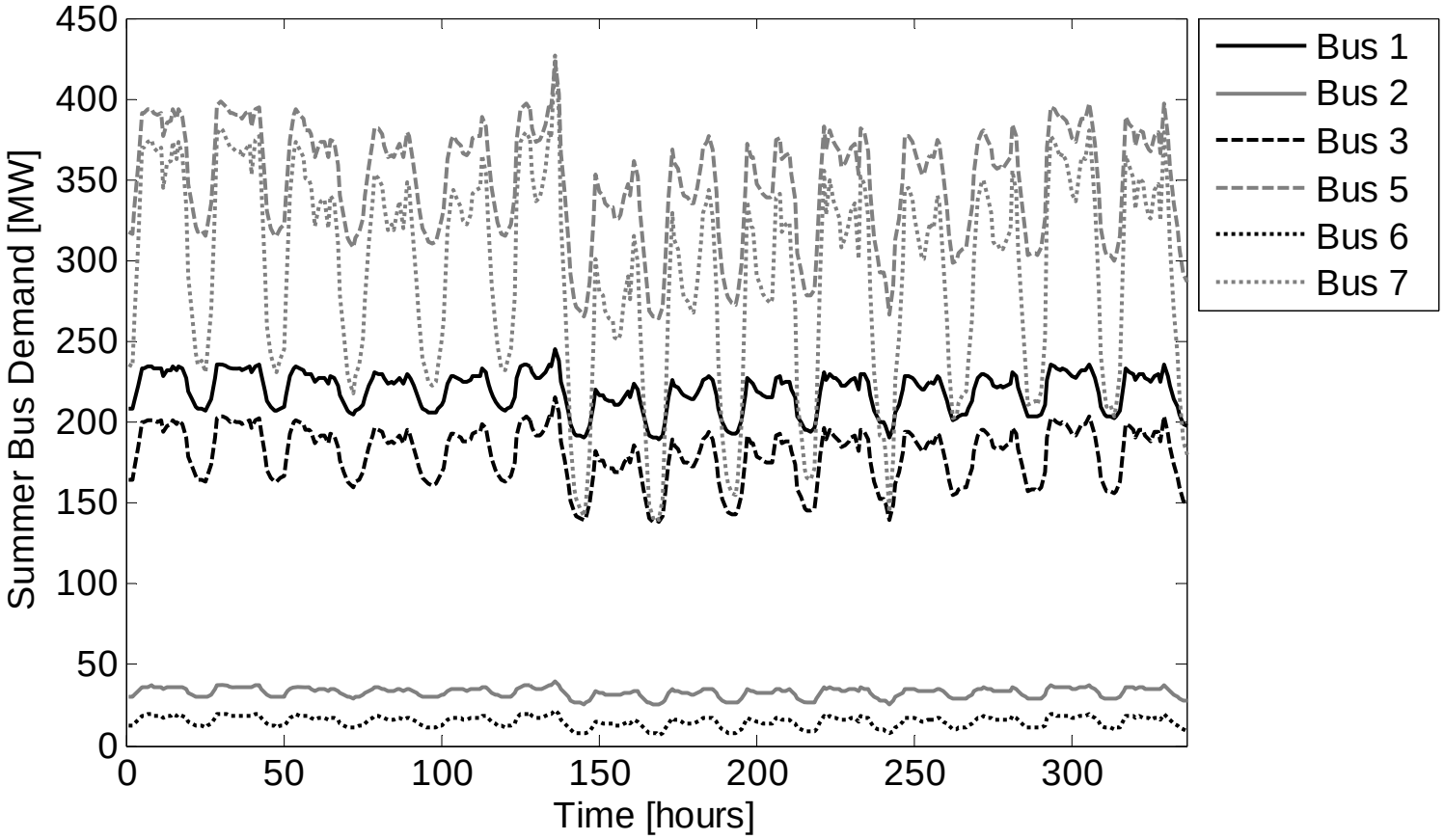
Summer Bus Demand [MW]
Time [hours]
0
50
100
150
200
250
300
350
400
450
Bus 1
Bus 2
Bus 3
Bus 5
Bus 6
Bus 7

Figure 6

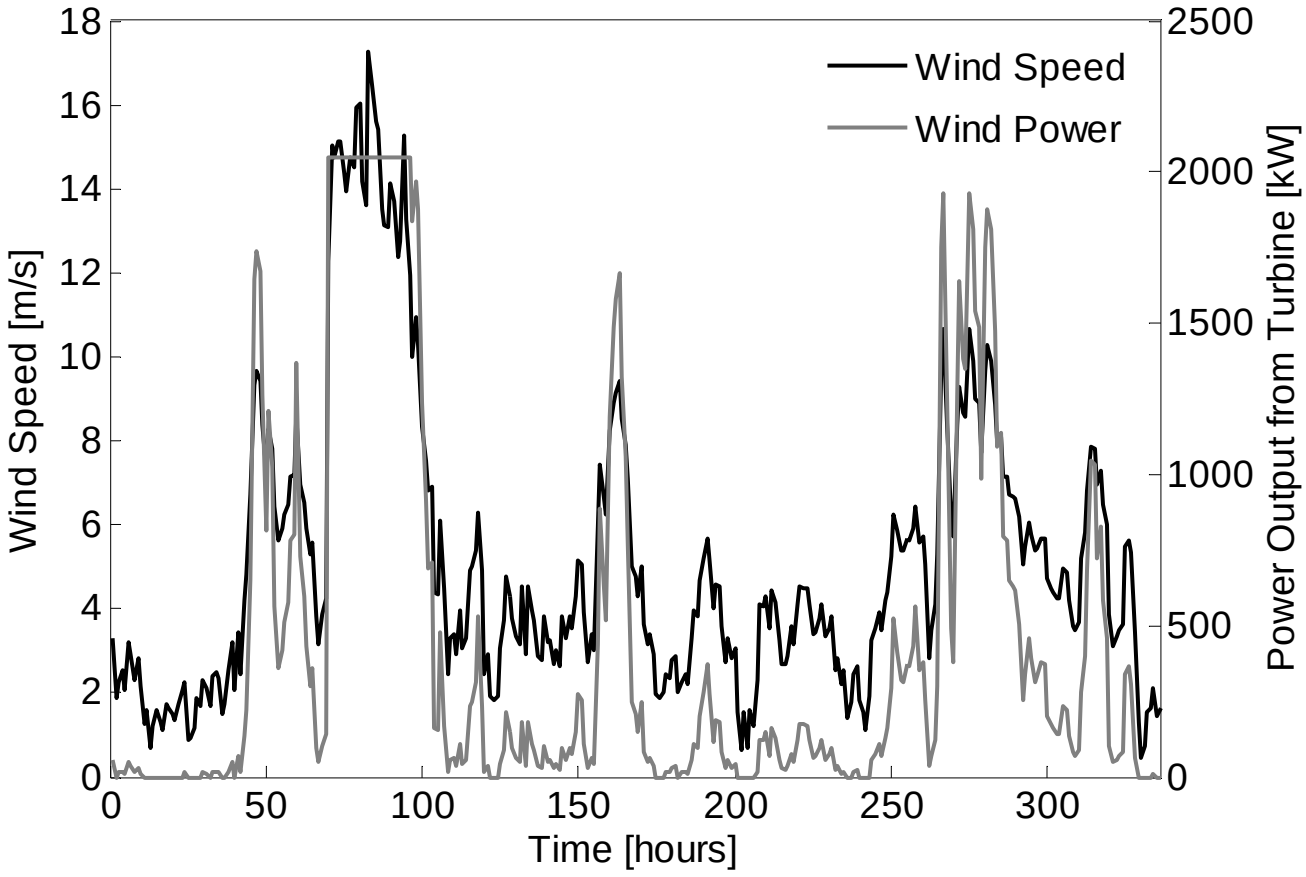
Wind Speed
Wind Power
Wind Speed [m/s]
Power Output from Turbine [kW]
Time [hours]
0
2
4
6
8
10
12
14
16
18
0
500
1000
1500
2000
2500
0
50
100
150
200
250
300

Figure 7

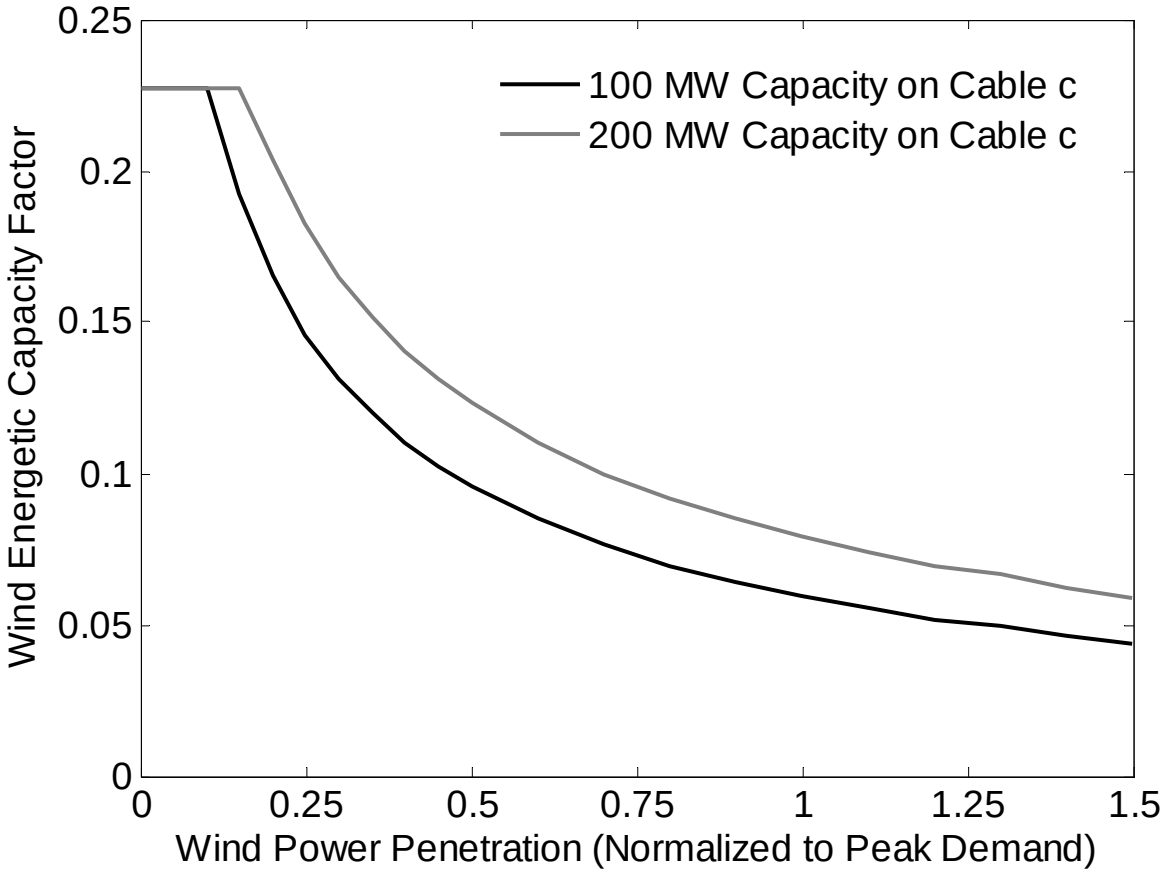
0.25
0.2
0.15
0.1
0.05
0
Wind Energetic Capacity Factor
100 MW Capacity on Cable c
200 MW Capacity on Cable c
0
0.25
0.5
0.75
1
1.25
1.5
Wind Power Penetration (Normalized to Peak Demand)

Figure 8

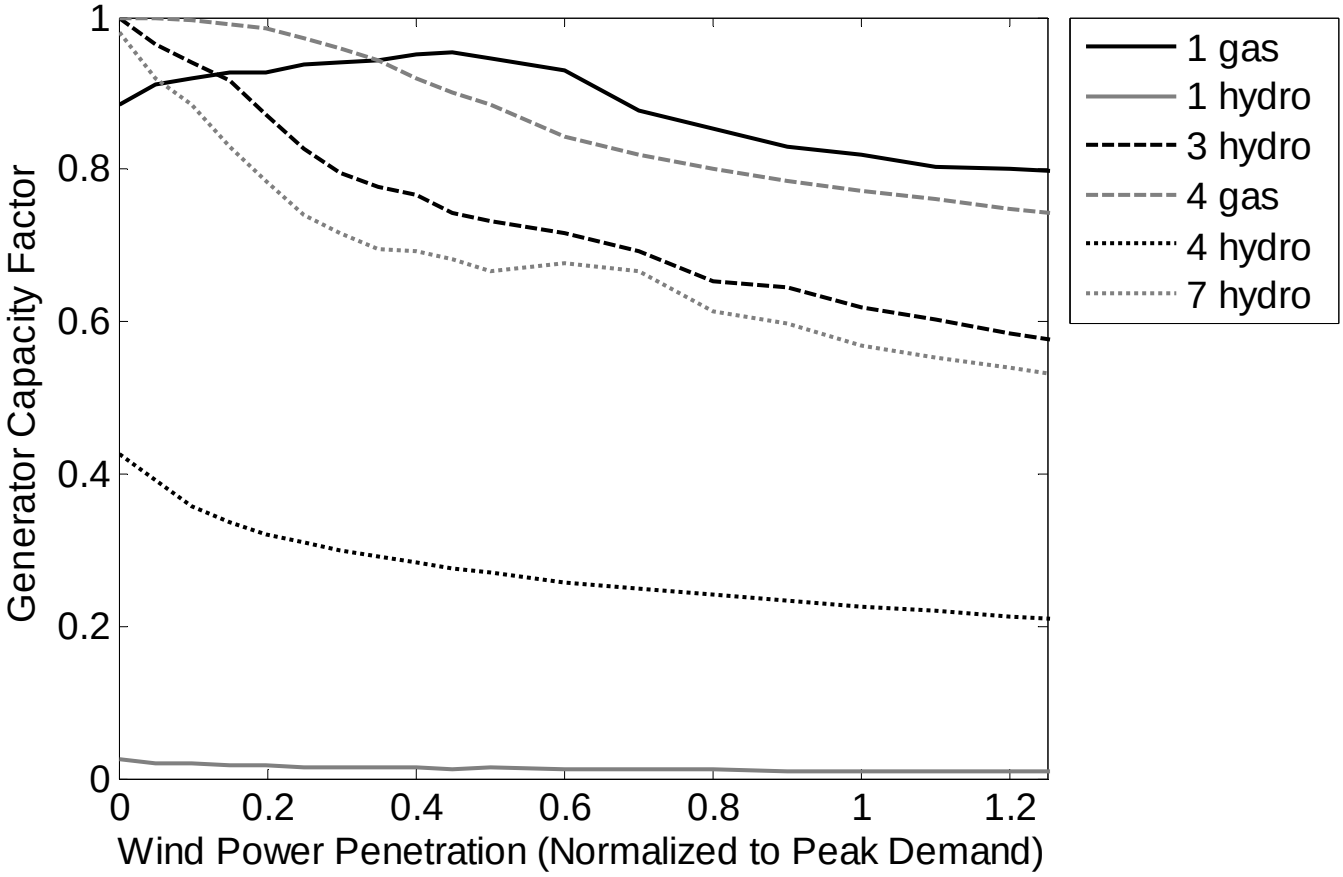
Generator Capacity Factor
Wind Power Penetration (Normalized to Peak Demand)
0
0.2
0.4
0.6
0.8
1
1.2
1 gas
1 hydro
3 hydro
4 gas
4 hydro
7 hydro

Figure 9

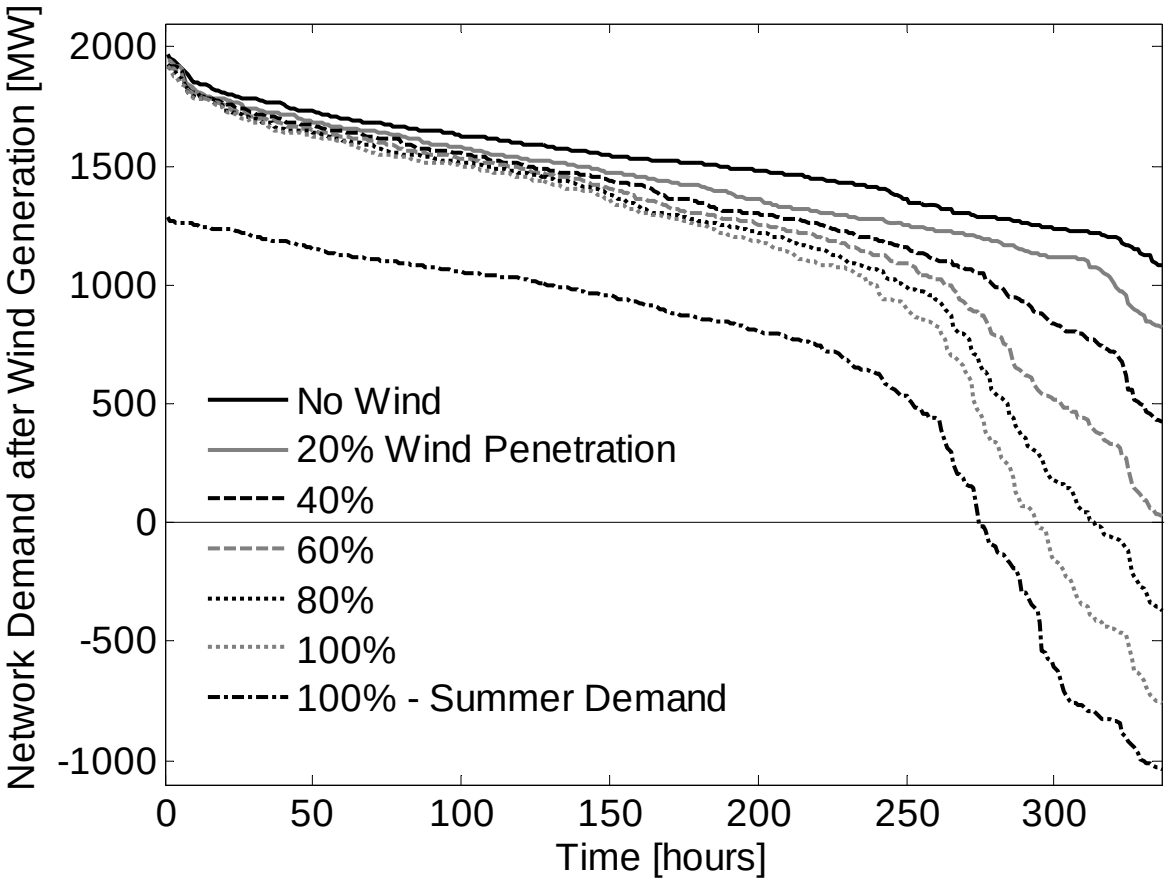
Network Demand after Wind Generation [MW]
2000
1500
1000
500
0
-500
-1000
0
50
100
150
200
250
300
Time [hours]
No Wind
20% Wind Penetration
40%
60%
80%
100%
100% - Summer Demand

Figure 10

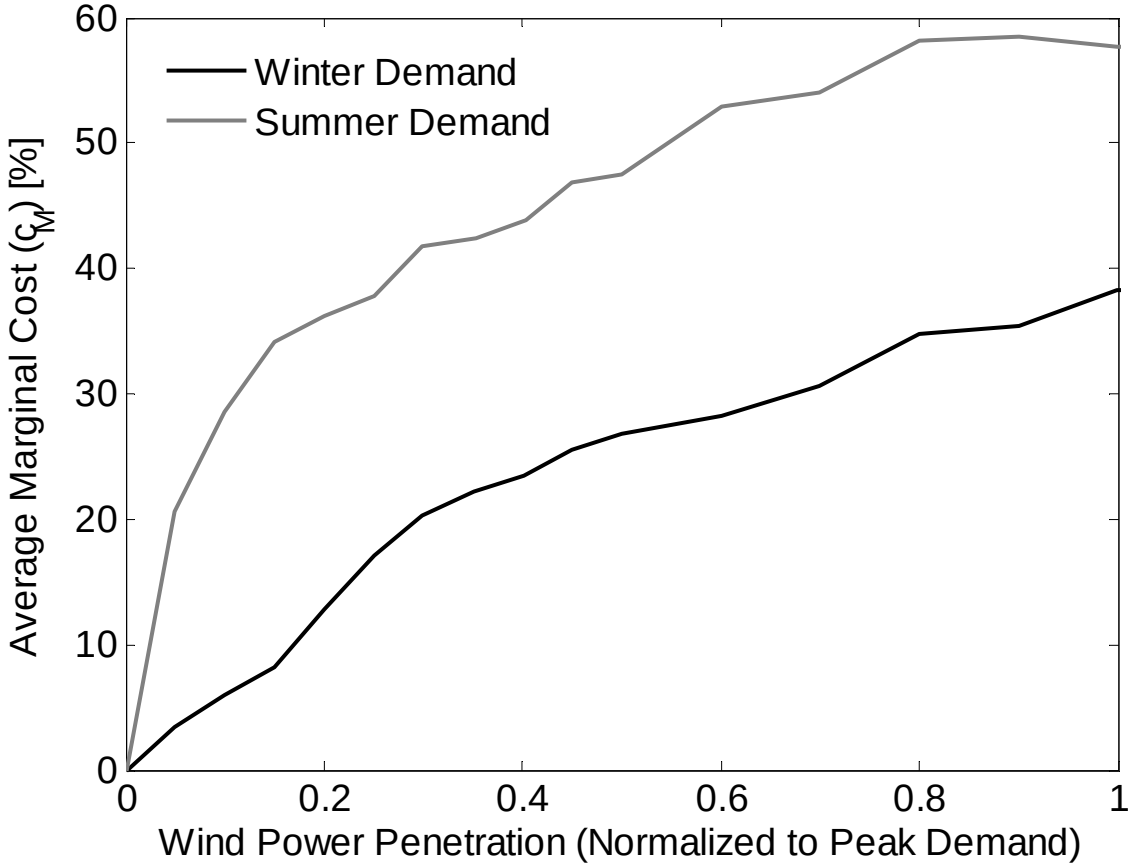
Winter Demand
Summer Demand
Average Marginal Cost (c_M) [%]
Wind Power Penetration (Normalized to Peak Demand)
0
10
20
30
40
50
60
0
0.2
0.4
0.6
0.8
1

Figure 11

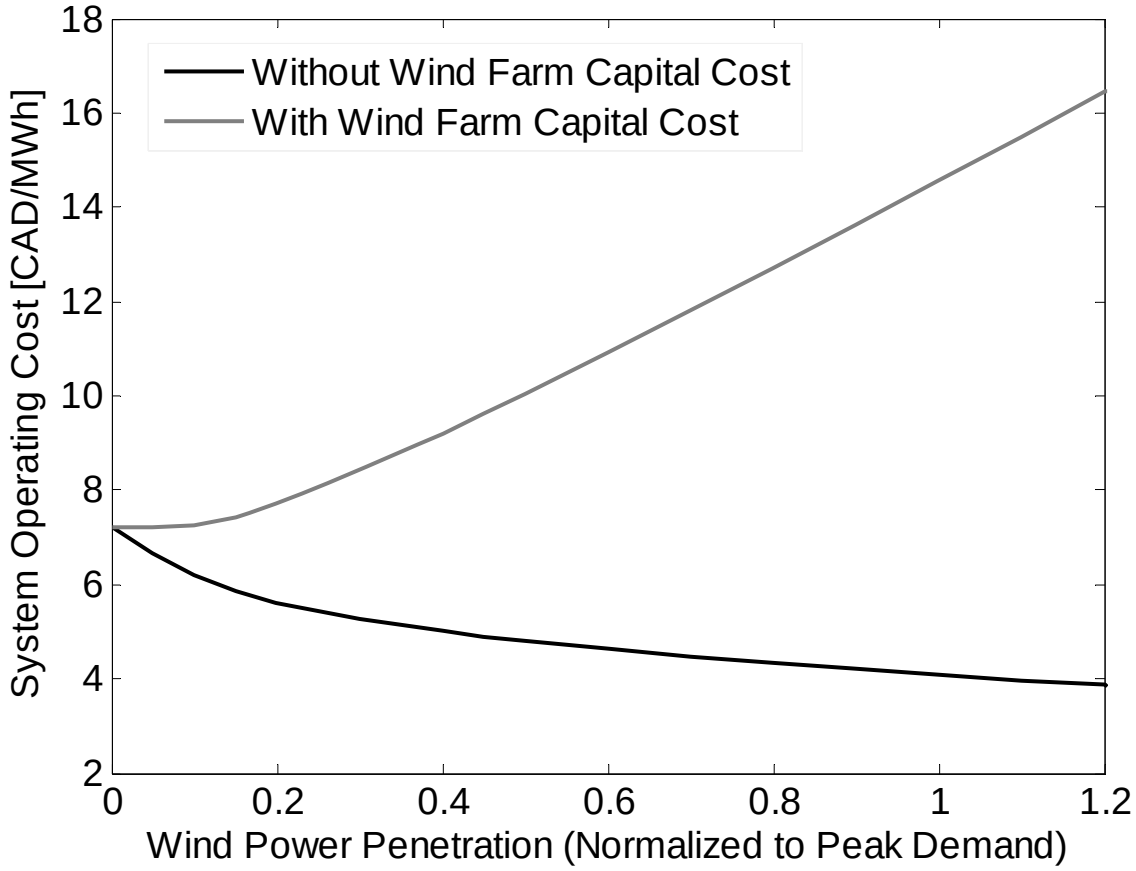
Without Wind Farm Capital Cost
With Wind Farm Capital Cost
System Operating Cost [CAD/MWh]
Wind Power Penetration (Normalized to Peak Demand)
18
16
14
12
10
8
6
4
2
0
0.2
0.4
0.6
0.8
1
1.2